Ab initio surface hopping simulation on dissociative recombination of H_3O^+

Megumi Kayanuma [a], Tetsuya Taketsugu [b,*], Keisaku Ishii [c]

[a] *Department of Chemistry, Ochanomizu University, Tokyo 112-8610, Japan*

[b] *Division of Chemistry, Graduate School of Science, Hokkaido University, Sapporo 060-0810, Japan*

[c] *Department of Chemical System Engineering, Graduate School of Engineering, University of Tokyo, Tokyo 113-8656, Japan*

Abstract

The dissociative recombination of H_3O^+ has been studied by the ab initio direct trajectory simulations at the state-averaged complete active space self-consistent field level to investigate tendency in the branching ratios of the dissociative products. Five electronic states of H_3O including two Rydberg states have been taken into account in the simulations, and nonadiabatic transitions among adiabatic states were taken into account by the Tully's fewest switches algorithm. It is verified that the highest energy products, OH + 2H, were generated in 87% of trajectories, while the most exothermic products, H_2O + H, were generated in 10% of trajectories.

* Corresponding author. Fax: +81 11 706 3535
E-mail address: take@sci.hokudai.ac.jp

1 Introduction

The dissociative recombination (DR) reaction is a combination of an electron and a positive molecular ion, which is followed by the dissociation into neutral molecules. The DR reaction proceeds via the direct mechanism or the indirect mechanism [1]. In the direct mechanism, the molecular system makes transitions directly from the electronic ground state of cation to the dissociative state of neutral molecule after capturing an electron. In the indirect mechanism, this transition proceeds via Rydberg states. In the interstellar medium, polyatomic ions are produced through ion-molecule reactions, and the DR process is one of the possible ways of neutralizing the ions. Through the DR reactions, polyatomic ions dissociate into different combinations of neutral atoms/molecules, and the study of the branching ratios of the DR reaction will help to understand the chemical evolution in interstellar clouds.

The possible mechanism to generate the water molecule in interstellar clouds may be the DR reaction of H_3O^+ with electrons [2-5],

$$H_3O^+ + e^- \rightarrow H_2O + H\,. \qquad (1)$$

In 1996, Andersen *et al.* provided the first evidence of this reaction, and showed that the efficiency was about 30% [6], which is in good agreement with observations of the $[H_2O]/[H_3O^+]$ ratio in the interstellar cloud. They investigated the branching ratios of the dissociative products from this reaction by using the heavy-ion storage ring ASTRID in Denmark [7,8], and reported the following ratio:

$$H_3O^+ + e^- \rightarrow \begin{cases} OH + 2H & (0.60) \\ H_2O + H & (0.25) \\ OH + H_2 & (0.14) \\ O + H_2 + H & (0.013) \end{cases} \qquad (2)$$

Ab initio molecular orbital calculations for the H_3O system have been carried out by several groups [9-13]. Ketvirtis and Simons [9] calculated the energy diagram for the H_3O^+/H_3O system, and found that the H_3O system produced by the DR reaction of $H_3O^+ + e^-$ can dissociate via several pathways to form H_2O ($X\ ^1A_1$) + H, OH ($X\ ^2\Pi$) + H_2, or OH ($X\ ^2\Pi$) + 2H. Although the reaction leading to the first products is the most exothermic, it does not constitute the product channel of largest branching ratio as observed experimentally. They suggested that the presence of sufficient excess internal energy in the nascent H_2O ($X\ ^1A_1$) causes a large fraction of this species to undergo further dissociation to OH ($X\ ^2\Pi$) + H, thereby enhancing the branching ratio of the latter product. Tachikawa [12] performed the full dimensional ab initio direct trajectory simulations for this DR reaction at the Hartree-Fock level. He investigated the dynamics on the ground state of H_3O by assuming vertical electron capture by H_3O^+, and showed that two reaction channels were involved in

this process. One channel is the process via a short-lived H_3O complex (5 ~ 60 fs), and the other channel is the process via a long-lived H_3O complex (> 200 fs), although the branching ratio for the second channel is negligibly small. Park *et al*. [13] calculated potential energy curves for the dissociation of the Rydberg H_3O radical into OH + H_2 by the Hartree-Fock and the singly and doubly excited configuration interaction methods. They showed that the ground $^2A_1$ potential energy curve of H_3O correlates to OH ($A\ ^2\Sigma^+$) + H_2($X\ ^1\Sigma_g^+$), while the first exited ^2E state of H_3O correlates to OH ($X\ ^2\Pi$) + H_2($X\ ^1\Sigma_g^+$) along the dissociation path of C_{2v} symmetry.

Very recently we have developed an ab initio direct trajectory code for the electronic excited states [14], and examined the DR reaction of $HCNH^+ + e^- \rightarrow$ HNC/HCN + H, which is also an important reaction in the interstellar chemistry. In this application we found that (1) HNC and HCN are generated with almost the same ratio, (2) the products, CN + 2H, are also generated, and (3) the isomerization between HNC and HCN can occur while the HCNH molecule descends through the electronic excited states. These results are in conformity with the experimental results and astronomical observations. In the present study, we apply our ab initio surface hopping trajectory method to the DR reaction of $H_3O^+ + e^-$, to verify the reaction mechanism of dissociations via the Rydberg and valence excited states, and to discuss the tendency in the branching ratios of dissociative products.

2. Ab initio calculations on electronic ground and excited states of H_3O

First we examined the energy levels of the ground and excited states of H_3O and the dissociative products from the DR reaction of $H_3O^+ + e^-$, *i.e.*, OH + 2H, H_2O + H, OH + H_2, and O + H_2 + H, by the state-averaged complete active space self-consistent field (SA-CASSCF) and the second order multireference perturbation theory (CASPT2) methods using the MOLPRO program package [15]. As the CASPT2 method, we have used a modified version developed by Celani and Werner [16], which is referred to as 'RS2C' in the MOLPRO program. Geometry optimization was carried out for H_3O^+ in the ground state at the CASSCF/6-311G(d,p) level with the full valence active space. For the thus optimized H_3O^+ geometry that belongs to the C_{3v} point group, the energetics were calculated for the neutral H_3O in the ground state (1 $^2A_1$), the first excited degenerate state (1 ^2E), and two Rydberg states (referred to as 2 $^2A_1$, 3 $^2A_1$) by the SA-CASSCF and CASPT2 methods with the 6-311G(d,p) basis sets augmented with Dunning-Hay's Rydberg functions of O atom (s type function with $\alpha_s = 0.032$ and p type function with $\alpha_p = 0.028$) [17] which is referred to as 6-311G(d,p)+Ryd(s,p). In these SA-CASSCF calculations, the full valence orbitals plus two Rydberg orbitals of O atom with a_1 symmetry (s and p_z orbitals where z-axis is taken as the C_3 axis of H_3O^+) were included in the active space (9 electrons in 9 orbitals), and five electronic states described above (1 $^2A_1$, 1 ^2E, 2 $^2A_1$, and 3 $^2A_1$) were equally averaged. For dissociative products, H_2O, OH, and H_2, we optimized geometrical structures by the CASSCF/6-311G(d,p) method (two states averaged SA-CASSCF was applied to OH ($^2\Pi$)) with the full valence active space, and calculated the relative energies by comparing with the energy of H_3O (1 $^2A_1$) evaluated by the state specific CASSCF and following CASPT2 calculations with 6-311G(d,p) basis sets. The energy for O (^3P) atom was also calculated by three states averaged SA-CASSCF and CASPT2 methods with 6-311G(d,p) basis sets, while the energy for H atom was set to an accurate value, -0.5 hartree. The relative energy of H_3O^+ (X $^1A_1$) and H_3O (1 $^2A_1$) was evaluated by the state specific CASSCF and CASPT2 methods with the full valence active space and 6-311G(d,p) basis sets.

In the ground state of H_3O^+, there are three unoccupied valence orbitals, $4a_1$ and $2e$ (two components), which are all anti-bonding orbitals between O and H atoms. In the valence electronic states of H_3O, an additional electron comes into one of these unoccupied orbitals of H_3O^+: $4a_1$ is singly occupied in the 1 $^2A_1$ ground state, while $2e$ is singly occupied in the 1 ^2E first-excited state. In SA-CASSCF and CASPT2 calculations, p_z-type Rydberg orbital is singly occupied in the 2 $^2A_1$ Rydberg state, while s-type Rydberg orbital is singly occupied in the 3 $^2A_1$ Rydberg state. According to the configuration interaction (CI) coefficients in the SA-CASSCF wavefunctions, the ground state 1 $^2A_1$ is largely mixed with the second Rydberg state 3 $^2A_1$. As to the other states, 1 ^2E and 2 $^2A_1$, the electronic states can be expressed by the single dominant configuration, respectively.

Figure 1 shows a summary of relative energies of (a) the related electronic states of H_3O (1 $^2A_1$, 1 ^2E, 2 $^2A_1$, 3 $^2A_1$) and H_3O^+ (X $^1A_1$), and (b) the dissociative products, OH + 2H, H_2O + H, OH + H_2,

and O + H_2 + H, at the SA-CASSCF (or CASSCF) and CASPT2 levels. The energy of H_3O ($1\ ^2A_1$) at the equilibrium structure of H_3O^+ ($X\ ^1A_1$) is taken as zero at both the SA-CASSCF and CASPT2 levels in Figs. 1a and 1b. The CASSCF method gives a poor estimation of the relative energy of H_3O^+ and H_3O because of different numbers of electrons. By including dynamical correlation effects in CASPT2 calculations, the CASSCF energies of the electronic states of H_3O are more lowered than the CASSCF energy of H_3O^+, resulting in more accurate energetics. Interestingly, the energy of H_3O^+ in the ground state was accidentally almost equal to that of the $3\ ^2A_1$ Rydberg state at the CASPT2 level.

As shown in Fig. 1, the CASSCF energies are in *qualitatively* agreement with the CASPT2 energies except for H_3O^+. For the dissociative products, the CASPT2 energy levels are higher by 12 ~ 26 kcal/mol than the CASSCF energy levels. Of course, it is better to employ the CASPT2 method in direct trajectory simulations for the DR reaction of $H_3O^+ + e^-$, but there is no code to evaluate analytical energy gradients and nonadiabatic coupling terms at the CASPT2 level in the current version of the Molpro program. Therefore, we decided to employ the SA-CASSCF method with the 6-311G(d,p)+Ryd(s,p) basis sets in the ab initio direct trajectory simulations. It is difficult to determine the branching ratio of the dissociative products quantitatively though the present simulations, but at least we can discuss the tendency in the dynamics. The SA-CASSCF active space and averaged states described above are also employed in the following dynamics simulations.

3. Ab initio surface hopping trajectory simulations

Ab initio surface hopping trajectory simulations have been carried out for the DR reaction of $H_3O^+ + e^-$. In the present simulation, the trajectory proceeds on a single adiabatic potential energy surface (PES), and the surface hopping is invoked around the nonadiabatic region where two adiabatic PES's are close to each other. The atomic positions and velocities are developed by the Newton equation of motion, while the electronic degree of freedom is developed by the time-dependent Schrödinger equation. The forces acting on the respective atoms are evaluated as the negatives of the energy gradients of the PES that are determined by *ab initio* molecular orbital calculations [18]. As the surface-hopping scheme, we have used the Tully's "fewest switches" algorithm [19].

In the present study we consider five electronic states of H_3O, *i.e.*, 1 ^{2}A, 2 ^{2}A, 3 ^{2}A, 4 ^{2}A, and 5 ^{2}A, in C_1 point group where 4 ^{2}A and 5 ^{2}A correspond to the Rydberg states. The electronic wavefunction Ψ is written as a function of time t,

$$\Psi(t) = c_1(t)\,\Psi_1 + c_2(t)\,\Psi_2 + c_3(t)\,\Psi_3 + c_4(t)\,\Psi_4 + c_5(t)\,\Psi_5, \tag{3}$$

where $c_k(t)$ and Ψ_k denote the electronic amplitude and eigenfunction, respectively, for the kth ^{2}A electronic state. Along the trajectory, the electronic amplitudes are also developed according to the time-dependent Schrödinger equation as

$$\begin{bmatrix} \dot{c}_1(t) \\ \dot{c}_2(t) \\ \dot{c}_3(t) \\ \dot{c}_4(t) \\ \dot{c}_5(t) \end{bmatrix} = \begin{pmatrix} \frac{V_1}{i\hbar} & -\mathbf{v}\cdot\mathbf{d}_{12} & -\mathbf{v}\cdot\mathbf{d}_{13} & -\mathbf{v}\cdot\mathbf{d}_{14} & -\mathbf{v}\cdot\mathbf{d}_{15} \\ \mathbf{v}\cdot\mathbf{d}_{12} & \frac{V_2}{i\hbar} & -\mathbf{v}\cdot\mathbf{d}_{23} & -\mathbf{v}\cdot\mathbf{d}_{24} & -\mathbf{v}\cdot\mathbf{d}_{25} \\ \mathbf{v}\cdot\mathbf{d}_{13} & \mathbf{v}\cdot\mathbf{d}_{23} & \frac{V_3}{i\hbar} & -\mathbf{v}\cdot\mathbf{d}_{34} & -\mathbf{v}\cdot\mathbf{d}_{35} \\ \mathbf{v}\cdot\mathbf{d}_{14} & \mathbf{v}\cdot\mathbf{d}_{24} & \mathbf{v}\cdot\mathbf{d}_{34} & \frac{V_4}{i\hbar} & -\mathbf{v}\cdot\mathbf{d}_{45} \\ \mathbf{v}\cdot\mathbf{d}_{15} & \mathbf{v}\cdot\mathbf{d}_{25} & \mathbf{v}\cdot\mathbf{d}_{35} & \mathbf{v}\cdot\mathbf{d}_{45} & \frac{V_5}{i\hbar} \end{pmatrix} \begin{bmatrix} c_1(t) \\ c_2(t) \\ c_3(t) \\ c_4(t) \\ c_5(t) \end{bmatrix}, \tag{4}$$

where $\mathbf{v}$ denotes atomic velocities, $\mathbf{d}_{kj}$ ($=<\Psi_k|\nabla|\Psi_j>$) denotes nonadiabatic coupling terms between the kth and jth electronic states, V_k is the adiabatic potential energy of the kth electronic state, and $\hbar$ is the Planck's constant divided by 2π. Nonadiabatic coupling terms are calculated by the SA-CASSCF method at each step. To reduce the computational cost, only the nonadiabatic coupling terms between neighboring states, $\mathbf{d}_{i,i+1}$, are evaluated, and others are set to zero. The probability of surface hopping from the kth to the jth electronic states within the time step of Δt are evaluated from the electronic amplitudes and nonadiabatic coupling terms as [19],

$$P_{kj}(t) = -2\mathrm{Re}\{(\mathbf{v}\cdot\mathbf{d}_{kj})\,c_k c_j^*\}\,\Delta t / |c_k|^2 . \tag{5}$$

The surface hopping is invoked when $P_{kj}(t)$ is greater than a uniform random number generated between 0 and 1. To conserve the total energy, the energy difference in the adiabatic potential energy before and after the surface hopping is converted to the kinetic energy. This conversion is performed

by scaling the component of atomic velocities in the direction of the nonadiabatic coupling vector in mass-weighted coordinates.

In the direct trajectory simulations, the SA-CASSCF calculations were carried out, step by step, in which five ^2A states are averaged with equal weights, and full-valence plus two Rydberg orbitals are included in the active space. The energy gradients and nonadiabatic coupling terms were calculated analytically by solving the coupled-perturbed multiconfigurational SCF equations for the relevant excited states. Such a direct trajectory approach requires extensive computational costs compared to the conventional trajectory simulations using potential energy functions. Using Pentium 4 3.2 GHz Linux PC computer, it took about 8 minutes CPU time to perform SA-CASSCF calculations for one step (including energy, gradients, and nonadiabatic coupling terms) along the trajectory. In this study, we have run 99 trajectories over a time length of up to 100 fs until bond dissociation occurs, with a fixed time step of 0.1 fs. The criteria for bond dissociations were determined arbitrarily, by checking energy variations along the respective bonds, as follows:

$$\begin{aligned}
&\mathrm{OH} + 2\mathrm{H} \quad \text{if two } r(\mathrm{OH}) > 3 \text{ Å, the other one } r(\mathrm{OH}) < 2 \text{ Å, and all } r(\mathrm{HH}) > 2 \text{ Å,} \\
&\mathrm{H_2O} + \mathrm{H} \quad \text{if one } r(\mathrm{OH}) > 3 \text{ Å and the other two } r(\mathrm{OH}) < 3 \text{ Å,} \\
&\mathrm{OH} + \mathrm{H_2} \quad \text{if two } r(\mathrm{OH}) > 3 \text{ Å, the other one } r(\mathrm{OH}) < 2 \text{ Å, and one } r(\mathrm{HH}) < 2 \text{ Å,} \\
&\mathrm{O} + \mathrm{H_2} + \mathrm{H} \quad \text{if all } r(\mathrm{OH}) > 3 \text{ Å and one } r(\mathrm{HH}) < 2 \text{ Å.}
\end{aligned} \tag{6}$$

The initial conditions for atomic positions and velocities are determined by the quasiclassical trajectory sampling [20] where zero-point vibrational energies are assigned, with random phases, to the respective normal modes of vibration of H_3O^+ in the electronic ground state. In the assignment of zero-point vibrational energies, the harmonic approximation was applied to non-totally symmetric modes, while the Morse approximation was applied to totally symmetric modes. The sum of zero-point vibrational energy was evaluated as 22.0 kcal/mol. Then, the molecule is placed on the adiabatic 5 ^{2}A PES of neutral H_3O, and the electronic amplitudes at $t = 0$ were set as,

$$c_{1A} = c_{2A} = c_{3A} = c_{4A} = 0,\ c_{5A} = 1. \tag{7}$$

It is noted that the H_3O^+ ground state and the 5 ^{2}A Rydberg state are accidentally degenerate with each other at the equilibrium point of H_3O^+ at the CASPT2 level, as described in the section 2. Thus, the initial conditions described above correspond to the situation that the H_3O^+ system make transitions to the 5 ^{2}A Rydberg state of H_3O without any increase or decrease of the energy on capturing an electron.

In the ab initio direct trajectory simulations with the SA-CASSCF method, we sometimes encounter a convergence problem in CASSCF calculations. This is because the SA-CASSCF wavefunction is restricted by the active space and the number of averaged states. The character of significant orbitals and low-lying electronic states can change in different regions of the configurational space. The difficulty as to change of significant orbitals can be reduced by including full valence orbitals in the active space. As to the electronic states, however, it is difficult to

determine the constant number of averaged states which avoids the convergence problem through the trajectory. In the present simulations where five electronic states are equally averaged in the SA-CASSCF calculations, the outer sixth electronic state often comes close to the inner fifth electronic state in energy, resulting in no convergence in the SA-CASSCF calculation. When this situation occurs while the molecule stays on the 5 ^{2}A state, we attempted to converge the SA-CASSCF calculation by applying several different orbital sets as initial guess; if these attempts failed, we increased the number of the averaged states to six temporarily, and continued the simulation until 5 ^{2}A and 6 ^{2}A states were separated sufficiently with each other; then, setting the number of averaged states to five again, we continued the simulation. When we encounter this situation while the molecule stays on the other states, 1 ^{2}A~ 4 ^{2}A, we decreased the number of averaged states one by one to continue the trajectory simulations. Even if such a convergence problem does not occur, we reduced the number of averaged states from 5 to 3 and eliminated two outer Rydberg orbitals from the active space after the molecule transits to the 3 ^{2}A state, to reduce the computational costs. When the potential energy shows a discontinuous change due to the change of the SA-CASSCF wavefunctions described above, we adjust the total energy of the system to keep the respective trajectories correctly continuous.

4. Results and discussion

In the present simulations, the converged SA-CASSCF energy for the 5 ^{2}A state ranges from 150 to 190 kcal/mol at initial stage in most trajectories. We have eliminated seven trajectories in which the initial SA-CASSCF energy is too high (190 ~ 330 kcal/mol), from the further analysis. Among 92 (= 99 – 7) trajectories, H_3O keeps its all OH bonds throughout (no bond cleavage) in 30 trajectories, while some bond dissociations occur during 100 fs in 62 trajectories. Among 62 trajectories, H_3O dissociates into OH + 2H in 54 trajectories (87%), into H_2O + H in 6 trajectories (10%), into OH + H_2 in one trajectory (1.5%), and into O + H_2 + H in one trajectory (1.5%). The thus estimated branching ratio is quantitatively different from the experimental one in Eq. (2), *i.e.*, (OH + 2H) : (H_2O + H) : (OH + H_2) : (O + H_2 + H) = 0.60 : 0.25 : 0.14 : 0.013. In our simulations, the estimated rates of the most exothermic products, H_2O + H, is relatively small, and also the products, OH + H_2, have been generated in only one trajectory. As shown in Fig. 1, the energy levels of these products, H_2O + H and OH + H_2, are much lower by about 100 kcal/mol than the other products, OH + 2H and O + H_2 + H. Since the molecular system starting from the second Rydberg state has too much excess energy, the dissociative products also should have an excess energy so that H_2O and OH further dissociate to the fragments as follows:

$$H_2O + H \rightarrow OH + H + H, \tag{8}$$

$$OH + H_2 \rightarrow O + H + H_2. \tag{9}$$

It is again noted that the CASSCF energies for the dissociative products are lower by 12~26 kcal/mol than the CASPT2 energies, and thus the dynamics simulation at the CASPT2 level should decrease the rate of OH + 2H, and increases the rates of H_2O + H and OH + H_2.

Figure 2 shows examples of variations of (a) the adiabatic potential energies, (b) the norm of the respective electronic amplitudes, (c) the inner product of the atomic velocity and the nonadiabatic coupling vector, and (d) the O-H interatomic distances in H_3O along the trajectory. This trajectory leads to the products, OH + 2H, where the first H atom leaves from O atom by 3.0 Å at t = 29.5 fs and the second H atom leaves at t = 32.8 fs as shown in Fig. 2d. The surface hopping occurs at t = 4.9 fs (5 ^{2}A → 4 ^{2}A), t = 7.9 fs (4 ^{2}A → 3 ^{2}A), and t = 10.9 fs (3 ^{2}A → 2 ^{2}A), which are denoted by dashed lines in Fig. 2a. After hopping to 3 ^{2}A state at t = 7.9 fs, the number of averaged states was reduced from 5 to 3 and the active space was reduced by eliminating two Rydberg orbitals as described above, so the adiabatic energies are not continuous at this point. The discontinuous point in adiabatic potential energies was also observed at t = 19.4 fs where the character of the 3 ^{2}A state changes with that of the 4 ^{2}A state that is not included in the state-average. The number of averaged states was reduced from 3 to 2 at t = 32.1 fs because of the convergence problem. When the surface hopping occurs, two adiabatic states come close to each other in energy as shown in Fig. 2a, the electronic amplitude changes drastically as shown in Fig. 2b, and the inner product of the atomic velocity and nonadiabatic coupling vector becomes large as shown in Fig. 2c. Therefore, the surface hopping is

invoked around the nonadiabatic region, although the Tully's fewest switches algorithm permits the molecule to make transitions between adiabatic states at any region in the configurational space.

As shown in Fig. 2a, the 1 ^{2}A, 2 ^{2}A, and 3 ^{2}A states become degenerate in the final stage. This is a common feature in energy profiles for trajectories leading to OH + 2H. This degeneracy can be understood by considering that the ground state of OH itself is a doubly-degenerate Π state, and also there is degeneracy due to the spin symmetry. The dissociative fragments, OH, H and H, are all doublet in spin multiplicity. Here we introduce the wavefunction to represent the electronic spin state of OH + H1 + H2 such as $\Psi(\alpha\alpha\alpha)$ where the first, second, and third α denote the spin function of OH, H1 and H2 fragments. Then the doublet state of OH + 2H can be represented in terms of $\Psi(\alpha\alpha\beta)$, $\Psi(\alpha\beta\alpha)$, and $\Psi(\beta\alpha\alpha)$. The linear combination,

$$\Psi(\alpha\alpha\beta)+\Psi(\alpha\beta\alpha)+\Psi(\beta\alpha\alpha), \tag{10}$$

belongs to the quartet state, while the other two combinations as

$$\Psi(\alpha\alpha\beta)-\Psi(\alpha\beta\alpha), \tag{11}$$

and

$$\Psi(\alpha\alpha\beta)+\Psi(\alpha\beta\alpha)-2\Psi(\beta\alpha\alpha), \tag{12}$$

belong to the doublet state. Thus, the degeneracy of the electronic ground state of OH (^{2}Π) + H (^{2}S) + H (^{2}S) are quadruple in the doublet state. Nonadiabatic transitions from the lower to the upper state occur only in such degenerate cases when the molecule dissociates into OH + 2H.

Figure 3 shows distributions of (a) the time when OH bond cleaves and (b) the time when surface hopping occurs. In Fig. 3a, H(1) and H(2) denote the first and second H atoms leaving from the molecular system, respectively. The peak time when the first H atom leaves is about $t \sim 25$ fs, while the peak time for the second H atom is about $t \sim 30$ fs. As shown in Fig. 3b, the first transition, 5 ^{2}A → 4 ^{2}A, was invoked at early stage (~ 15 fs), and the following transitions (4 ^{2}A → 3 ^{2}A → 2 ^{2}A → 1 ^{2}A) have completed at around $t = 50$ fs in most cases. The dissociation into H_2O + H occurs on the 1 ^{2}A ground state in all cases, while the dissociation into OH + 2H occurs on the 1 ^{2}A ground state in 32 trajectories, on the 2 ^{2}A state in 17 trajectories, and on the 3 ^{2}A state in 5 trajectories. This difference can be related to the degeneracy in the potential energy surfaces for OH + 2H described above, and when the dissociation to OH + 2H occurs in the 2 ^{2}A or 3 ^{2}A excited states, these excited states are already degenerate with the ground state 1 ^{2}A. In such a degenerate case, the upward surface-hopping was observed in some trajectories, i.e., 2 ^{2}A → 3 ^{2}A in three trajectories, and 1 ^{2}A → 2 ^{2}A in seven trajectories.

There is one trajectory leading to the products, O + H_2 + H, in which two H atoms attempt to leave after the transition to 2 ^{2}A at $t = 8.1$ fs, and then one of them dissociates smoothly while another one dissociates slowly; the latter H atom binds later with the third H atom which has also left from the O atom, resulting in generation of an H_2 molecule. The first H atom leaves from O atom by 3.0 Å at $t = 21.3$ fs, while two other H atoms leave by 3.0 Å almost simultaneously at $t = 46.0 \sim 47.5$ fs. In

this case the surface hoppings from 5 ^{2}A to 1 ^{2}A via 4 ^{2}A, 3 ^{2}A, and 2 ^{2}A states have completed at t = 14.8 fs. The vibrational energy for the leaving H_2 molecule was calculated as about 47 kcal/mol. There is also one trajectory leading to OH + H_2, in which two H atoms start to dissociate simultaneously after the molecule makes a transition to 2 ^{2}A state at t = 30.1 fs, and then bind with each other. The H_2 molecule leaves from O atom by 3.0 Å at t = 55.9 fs. The surface hopping from 5 ^{2}A to 1 ^{2}A via 4 ^{2}A, 3 ^{2}A, and 2 ^{2}A states have completed at t = 51.7 fs. The vibration energy was calculated as about 40 kcal/mol for OH molecule, and as 77 kcal/mol for H_2 molecule.

We have further analyzed the motions of dissociative molecules by partitioning the total energy to those of the respective translational, rotational, and vibrational modes of the fragments. The excess energy of the H_3O system having the zero-point vibrational energy in the second Rydberg state is evaluated as 176 kcal/mol relative to the dissociation limit of H_2O + H, and as 70 kcal/mol relative to the dissociation limit of OH + 2H at the CASSCF level, which are distributed to the energies of the respective fragments in the final stage. It is noted that these numbers are reduced to 159 and 46 kcal/mol for H_2O + H and OH + 2H, respectively, at the CASPT2 level. When the molecule dissociates into H_2O + H, the translational energies of H_2O and H are distributed with the ratio of the inverse of mass of the fragments according to the conservation rule of momentum. There were six trajectories that lead to the products, H_2O + H, in which the translational energies were estimated in the range of 9 ~ 81 kcal/mol. The remaining energies, 95 ~ 167 kcal/mol, should be given to the rotational and vibrational modes of H_2O although H_2O should have at least 13.3 kcal/mol as the zero-point vibrational energy. The energy of H_2O relative to that of OH + H is evaluated as 106 kcal/mol at the CASSCF level. Thus, the H_2O molecule having more than 106 kcal/mol as the internal energy can possibly dissociate into OH + H if the energy comes together to one OH bond of H_2O. Thus, three of six trajectories leading to H_2O + H can further dissociate into OH + 2H.

Figure 4 shows distributions of (a) translational, (b) rotational, and (c) vibrational energies of the produced OH molecule and of (d) translational energies of H atoms for 54 trajectories leading to OH + 2H. Here, the total number of H atoms is 108 in Fig 4d since there are two H atoms in each trajectory. The OH vibrational energy was estimated from the O-H vibrational amplitude, based on the potential energy curve of OH molecule determined at the two-state averaged SA-CASSCF/6-311G(d,p) level. As shown in these figures, most of the energy was distributed to the OH vibrational energy and translational energy of H atoms. The translational energy of H atoms varies in the range of 0 ~ 40 kcal/mol in most cases. In OH molecule, the translational energy is less than 4 kcal/mol, and the rotational energy is less than 1 kcal/mol in most cases. The OH vibrational energy varies in the range of 0 ~ 65 kcal/mol. It is noted that the OH binding energy was calculated as about 80 kcal/mol at the SA-CASSCF level.

5. Concluding remarks

Ab initio direct trajectory simulations have been carried out for the dissociative recombination reaction, $H_3O^+ + e^-$, at the SA-CASSCF level, to examine the tendency in the branching ratio of the dissociative products, and also to investigate the dynamical processes with nonadiabatic transitions among adiabatic states. The surface hopping mechanism was taken into account by the Tully's fewest switches algorithm, which permits nonadiabatic transitions between adiabatic states at any region in the configurational space. The energy diagram for the compounds included in the reactions, i.e., the ground state of H_3O^+, the ground and excited states of H_3O, and the ground states of OH + 2H, H_2O + H, OH + H_2, and O + H_2 + H have been examined at the CASSCF and CASPT2 levels. We have included two Rydberg states of H_3O in the present calculations, which should play a significant role in the indirect process of the dissociative recombination reaction. It is verified that CASSCF and CASPT2 methods give the qualitatively similar energetics except for the energy level of H_3O^+, although the CASSCF energies of the dissociative products were higher by 12 ~ 26 kcal/mol than the CASPT2 energies. We have run 99 trajectories with the initial conditions that zero-point vibrational energies are given to the respective normal vibrational modes of H_3O^+ with random phases, and the molecule is put on the second Rydberg state of H_3O that is accidentally degenerate to the cationic ground state. In the present simulations, the surface hopping was observed in the relatively early stage less than 30 fs in most cases, and the rates of the respective dissociative products are estimated as (OH + 2H) : (H_2O + H) : (OH + H_2) : (O + H_2 + H) = 0.87 : 0.10 : 0.015 : 0.015, while the corresponding experimental rates were reported as 0.60 : 0.25 : 0.14 : 0.013. The rate of exothermic products is small compared to the experimental ones, but the order in the ratio is reproduced. The direct trajectory simulations including dynamical correlation effects will be required to obtain more quantitative branching ratio.

Acknowledgments

The present work was supported by an allocation of computing resources of SGI2800 from the Institute of Statistical Mathematics in Tokyo.

References

[1] S. L. Guberman, in Dissociative Recombination of Molecular Ions with Electrons, ed. S. L. Guberman, Kluwer Academic / Plenum Publishers, New York, pp1, 2003.

[2] E. F. Van Dishoeck, in Molecular Astrophysics, ed. T. W. Hartquist, Cambridge University Press, Cambridge, UK, pp55, 1990.

[3] T. J. Miller, in Molecular Astrophysics, ed. T. W. Hartquist, Cambridge University Press, Cambridge, UK, pp115, 1990.

[4] D. R. Bates, in Molecular Astrophysics, ed. T. W. Hartquist, Cambridge University Press, Cambridge, UK, pp211, 1990.

[5] D. A. Neufeld, S. Lepp, G. J. Melnick, Astrophys. J. Suppl. Ser. 100 (1995) 132.

[6] L. H. Andersen, O. Heber, D. Kella, H. B. Pedersen, L. Vejby-Christensen, D. Zajfman, Phys. Rev. Lett. 77 (1996) 4891.

[7] L. Vejby-Christensen, L. H. Andersen, O. Heber, D. Kella, H. B. Pedersen, H. T. Schmit, D. Zajfman, Astrophys. J. 483 (1997) 531.

[8] M. J. Jensen, R. C. Bilodeau, C. P. Safvan, K. Seiersen, L. H. Andersen, H. B. Pedersen, O. Heber, Astrophys. J. 543 (2000) 764.

[9] A. E. Ketvirtis, J. Simons, J. Phys. Chem. A 103 (1999) 6552.

[10] P. W. McLoughlin, G. I. Gellene, J. Phys. Chem. 96 (1992) 4396.

[11] D. Talbi, R. P. Saxon, J. Chem. Phys. 91 (1989) 2376.

[12] H. Tachikawa, Phys. Chem. Chem. Phys. 2 (2000) 4327.

[13] J. K. Park, B. G. Kim, I. S. Koo, Chem. Phys. Lett. 356 (2002) 63.

[14] T. Taketsugu, A. Tajima, K. Ishii, T. Hirano, Astrophys. J. 608 (2004) 323.

[15] MOLPRO, a package of ab initio programs designed by H.-J. Werner, P. J. Knowles, version 2002.1, R. D. Amos, A. Bernhardsson, A. Berning, P. Celani, D. L. Cooper, M. J. O. Deegan, A. J. Dobbyn, F. Eckert, C. Hampel, G. Hetzer, P. J. Knowles, T. Korona, R. Lindh, A. W. Lloyd, S. J. McNicholas, F. R. Manby, W. Meyer, M. E. Mura, A. Nicklass, P. Palmieri, R. Pitzer, G. Rauhut, M. Schutz, U. Schumann, H. Stoll, A. J. Stone, R. Tarroni, T. Thorsteinsson, H.-J. Werner.

[16] P. Celani, H.-J. Werner, J. Chem. Phys. 112 (2000) 5546.

[17] T. H. Dunning Jr., P. J. Hay, in Methods of electronic structure theory, vol. 2, ed. H. F. Schaefer III, Plenum Press, 1977.

[18] M. S. Gordon, G. Chaban, T. Taketsugu, J. Phys. Chem. 100 (1996) 11512.

[19] J. C. Tully, J. Chem. Phys. 93 (1990) 1061.

[20] G. H. Peslherbe, H. Wang, W. L. Hase, in Advances in Chemical Physics, vol. 105, eds. D. M. Ferguson, J. I. Siepman, D. G. Truhlar, Wiley, New York, pp171, 1999.

Figure caption

Fig. 1. Relative energies of (a) the electronic states of H_3O ($1\ ^2A_1$, $1\ ^2E$, $2\ ^2A_1$, $3\ ^2A_1$) and $H_3O^+(X\ ^1A_1)$, and (b) the dissociative products, OH + 2H, H_2O + H, OH + H_2, and O + H_2 + H, at the SA-CASSCF (or CASSCF) and CASPT2 levels.

Fig. 2. Variation of (a) the adiabatic potential energies, (b) the norm of the respective electronic amplitudes, (c) the inner product of the atomic velocity and nonadiabatic coupling vector, and (d) the O-H interatomic distances along the trajectory.

Fig. 3. Distributions of (a) the lifetime of the trajectory until bond dissociations occur and (b) the time step when surface hopping in the descending way occurs. In part (a), H(1) and H(2) indicate the first and second hydrogen atoms departing from OH.

Fig. 4. Distribution of (a) translational, (b) rotational, and (c) vibrational energies of the produced OH molecule and of (d) translational energies of H atoms for 54 trajectories leading to OH + 2H.

Figure

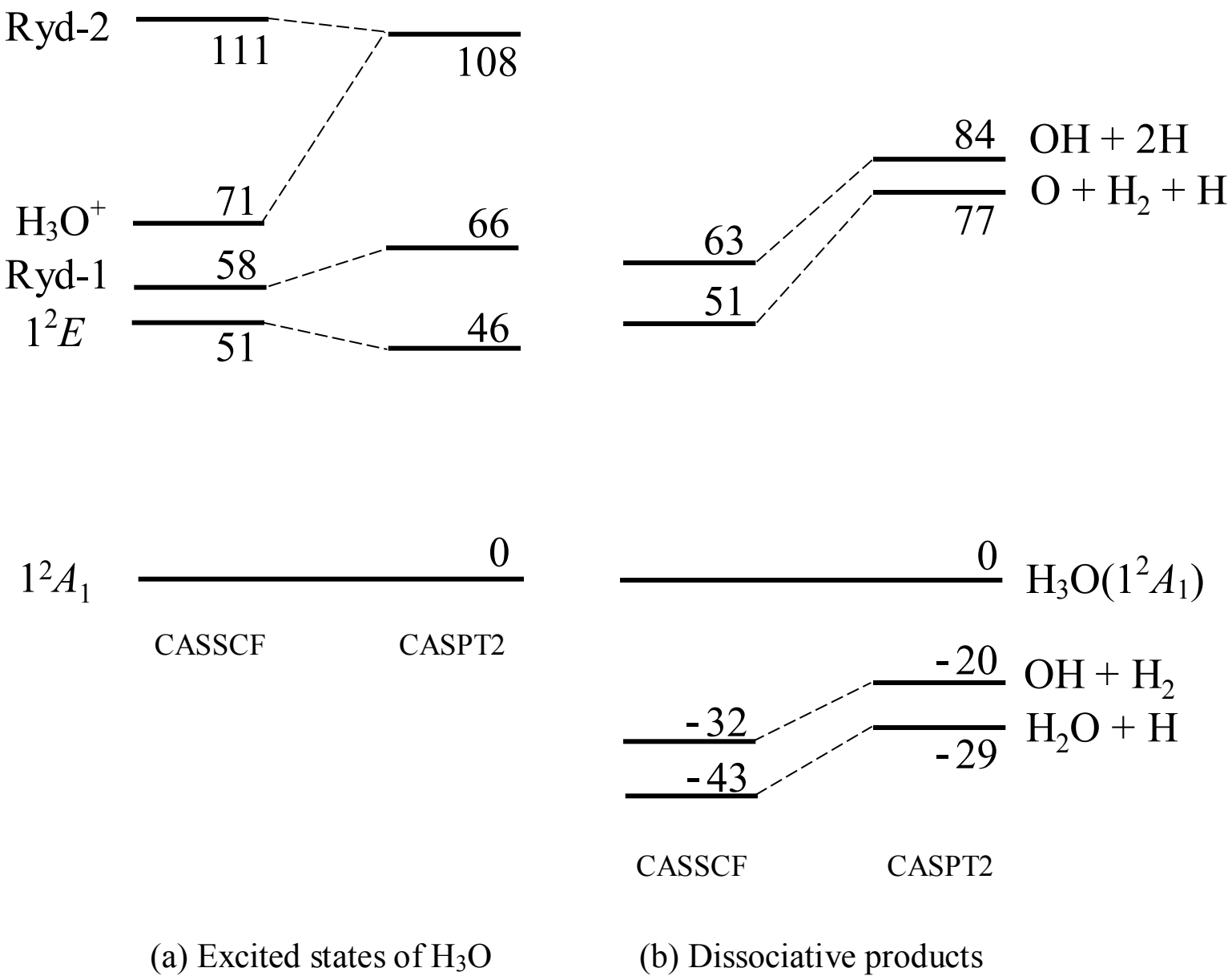

(a) Excited states of H_3O (b) Dissociative products

Fig.1. “Ab initio direct trajectory …” by Kayanuma et al.

Figure

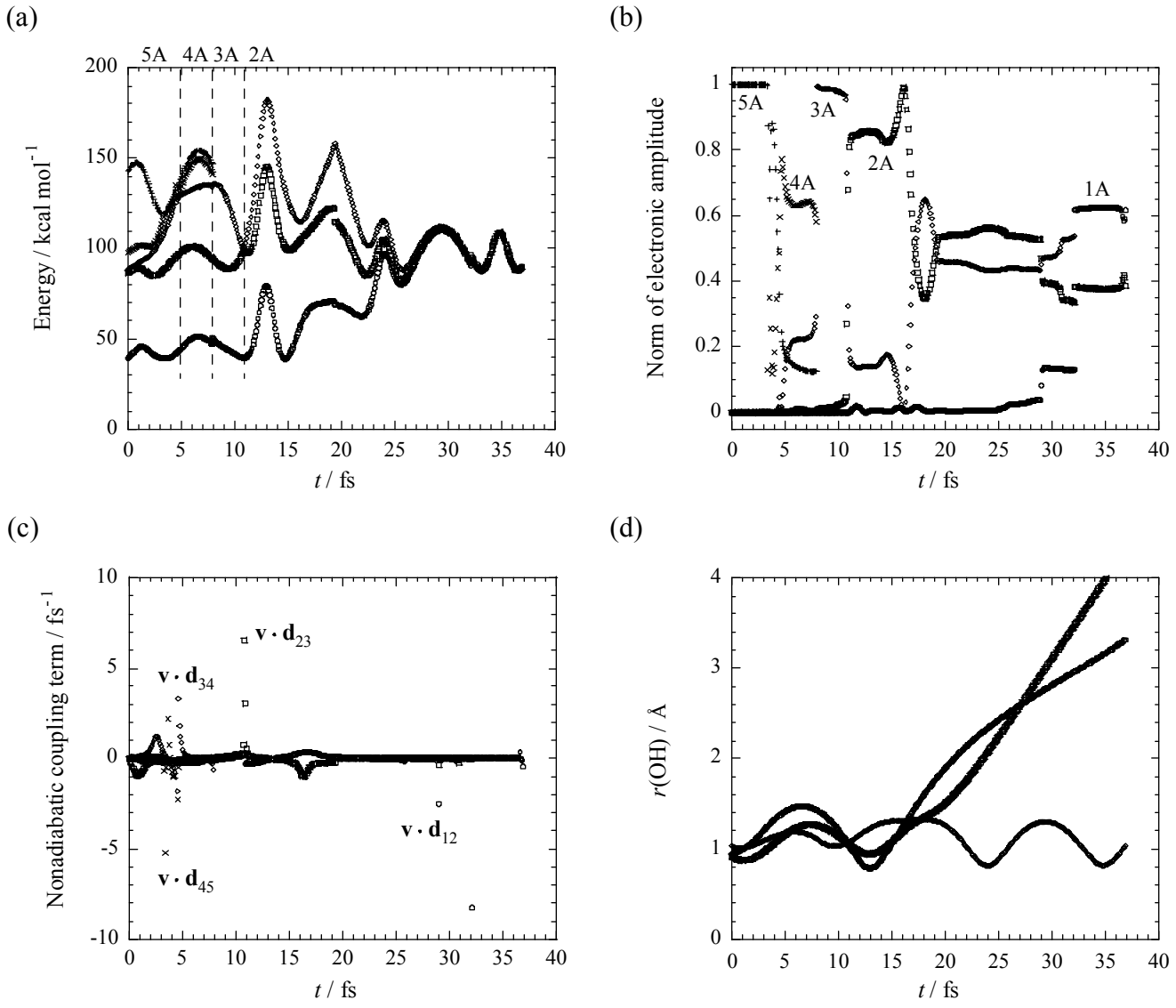

Fig.2. “Ab initio direct trajectory …” by Kayanuma et al.

Figure

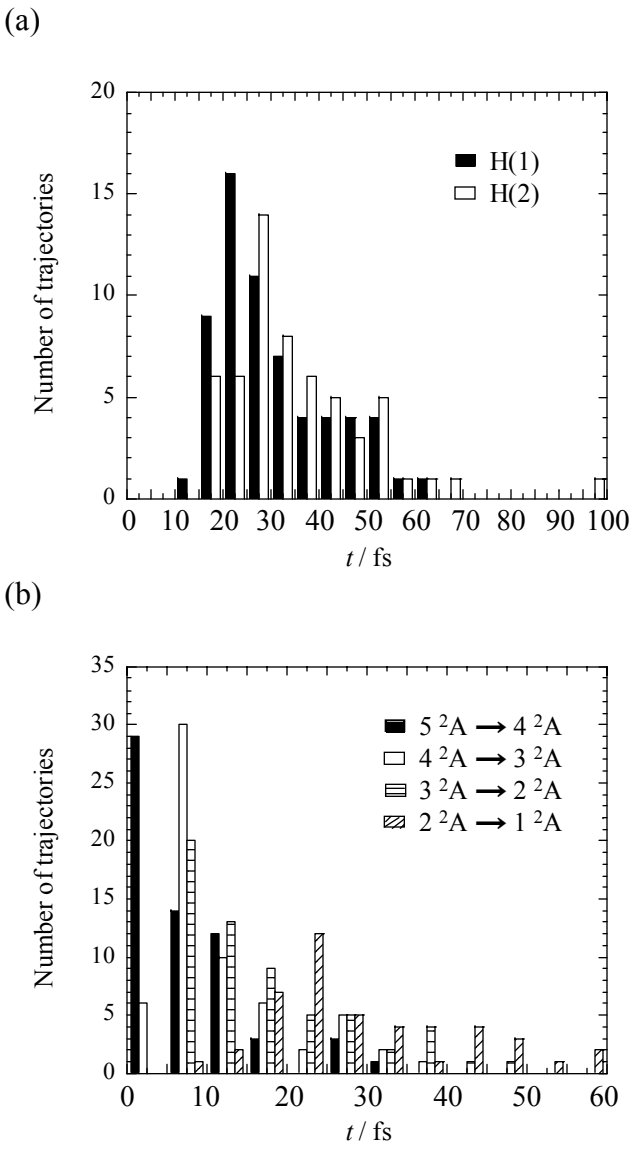

Fig.3. “Ab initio direct trajectory …” by Kayanuma et al.

Figure

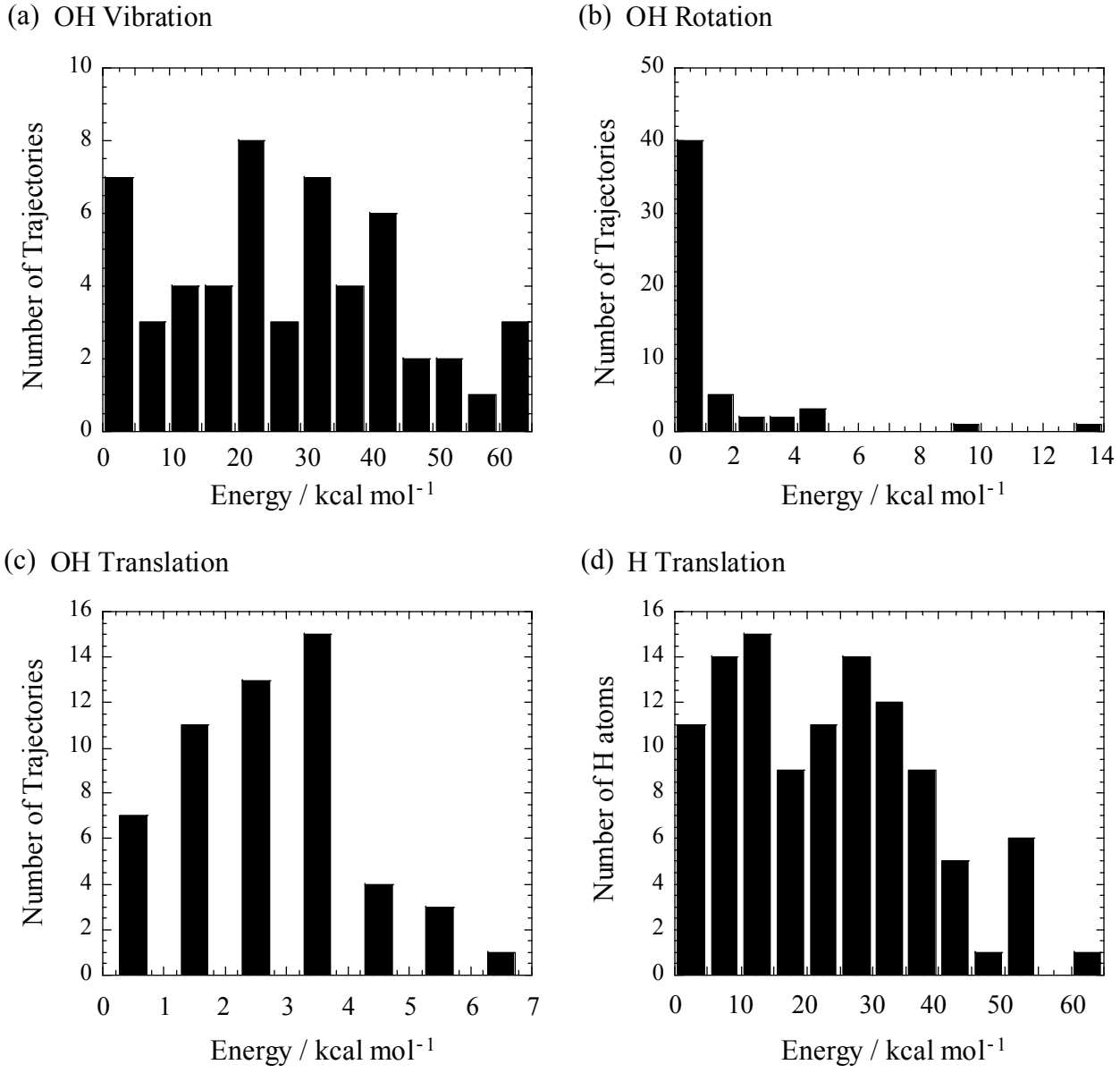

Fig.4. “Ab initio direct trajectory …” by Kayanuma et al.